PAPER

Orthogonal Multi-Carrier DS-CDMA with Frequency-Domain Equalization

Ken TANAKA[†a)], **Hiromichi TOMEBA**[†], ***Student Members***, ***and*** **Fumiyuki ADACHI**[†], ***Fellow***

SUMMARY Orthogonal multi-carrier direct sequence code division multiple access (orthogonal MC DS-CDMA) is a combination of orthogonal frequency division multiplexing (OFDM) and time-domain spreading, while multi-carrier code division multiple access (MC-CDMA) is a combination of OFDM and frequency-domain spreading. In MC-CDMA, a good bit error rate (BER) performance can be achieved by using frequency-domain equalization (FDE), since the frequency diversity gain is obtained. On the other hand, the conventional orthogonal MC DS-CDMA fails to achieve any frequency diversity gain. In this paper, we propose a new orthogonal MC DS-CDMA that can obtain the frequency diversity gain by applying FDE. The conditional BER analysis is presented. The theoretical average BER performance in a frequency-selective Rayleigh fading channel is evaluated by the Monte-Carlo numerical computation method using the derived conditional BER and is confirmed by computer simulation of the orthogonal MC DS-CDMA signal transmission.

key words: *orthogonal MC DS-CDMA, frequency-domain equalization, frequency diversity gain*

1. Introduction

High speed data transmission of over 100 Mbps is required for the next generation mobile communication systems. However, the mobile channel is characterized by frequency-selective fading channel, and therefore, the bit error rate (BER) performance significantly degrades due to severe inter-symbol interference [1]–[4]. To avoid the adverse effect of frequency-selective fading, much attention has been paid to the multi-carrier technique, known as multi-carrier code division multiple access (MC-CDMA) [5]–[8]. In MC-CDMA, frequency-domain spreading is combined with orthogonal frequency division multiplexing (OFDM). On the other hand, in direct sequence code division multiple access (DS-CDMA), time-domain spreading is used. Good BER performance can be achieved by using frequency-domain equalization (FDE) based on minimum mean square error (MMSE) criterion, since the frequency diversity gain can be obtained [9], [10].

Another CDMA technique is orthogonal multi-carrier direct sequence code division multiple access (orthogonal MC DS-CDMA) which is a combination of OFDM and time-domain spreading (this is called orthogonal MC DS-CDMA type-II in [5]). In orthogonal MC DS-CDMA, DS-CDMA is applied to each OFDM subcarrier to transmit different data symbols using different subcarriers. All subcarriers for each user can be assigned the same user-specific spreading code. Orthogonal MC DS-CDMA cannot obtain the frequency diversity gain. Recently, variable spreading factor-orthogonal frequency and code division multiplexing (OFCDM) was proposed that uses both frequency- and time-domain spreading [11], [12]. In OFCDM, time-domain spreading is prioritized rather than frequency-domain spreading. OFCDM using time-domain spreading only is equivalent to the conventional orthogonal MC DS-CDMA. In this paper, we propose a new orthogonal MC DS-CDMA which can obtain the frequency diversity gain through the use of FDE. Broadband wireless packet access will be the core technology for the next generation mobile communications systems. Hybrid automatic repeat request (HARQ) technique is an indispensable technique [13]. HARQ using incremental redundancy (IR) strategy is known to achieve the high throughput performance [14]. Since the proposed orthogonal MC DS-CDMA with FDE can obtain the frequency diversity gain without using the frequency-domain spreading, it can increase the throughput of HARQ with IR strategy.

The remainder of this paper is organized as follows. Sect. 2 describes the transmission system model of the proposed orthogonal MC DS-CDMA with FDE. The conditional BER analysis is presented in Sect. 3. In Sect. 4, the theoretical average BER performance in a frequency-selective Rayleigh fading channel is numerically evaluated by Monte-Carlo numerical computation method using the derived conditional BER expression and is confirmed by computer simulation. The throughput performance improvement of HARQ with IR strategy is also discussed. Sect. 5 offers some conclusions.

2. Orthogonal MC DS-CDMA with FDE

In orthogonal MC DS-CDMA, all modulated subcarriers are orthogonal when observed over the chip period. However, if the observation interval is extended beyond the chip period, the spectrum of each DS-CDMA signal transmitted on different orthogonal subcarrier is spread (of course, its spectrum becomes null at different subcarrier frequencies). This can be exploited to get the frequency diversity gain although frequency-domain spreading is not used. We apply an $N_f \times N_c$-point fast Fourier transform (FFT) to the received orthogonal MC DS-CDMA to transform it into the frequency-domain signal with $N_f \times N_c$ frequency compo-

Manuscript received December 7, 2006.
Manuscript revised August 26, 2007.

[†]The authors are with the Department of Electrical and Communication Engineering, Graduate School of Engineering, Tohoku University, Sendai-shi, 980-8579 Japan.
a) E-mail: tanaka@mobile.ecei.tohoku.ac.jp

DOI: 10.1093/ietcom/e91–b.4.1055

nents for performing FDE, where N_f and N_c denote an integer number and the number of subcarriers of orthogonal MC DS-CDMA signal, respectively. After performing FDE, the equalized frequency-domain signal is transformed back to the time-domain signal by $N_f \times N_c$-point inverse FFT (IFFT). Then, we apply the conventional orthogonal MC DS-CDMA demodulation. Through a series of $N_f \times N_c$-point FFT, FDE, $N_f \times N_c$-point IFFT, and conventional orthogonal MC DS-CDMA demodulation, we can get the frequency diversity gain.

2.1 Overall Transmission System

The transmitter/receiver structure of orthogonal MC DS-CDMA with FDE is illustrated in Fig. 1. At the transmitter, a binary data sequence is transformed into a data modulated symbol sequence, which is spread by a user-specific spreading sequence $\{c(n);\ n = 0{\sim}SF{-}1\}$. Then, N_c-point IFFT is applied chip-by-chip to generate the orthogonal MC DS-CDMA signal with N_c subcarriers. The last N_g samples of an $N_f \times N_c$-sample block (or N_f OFDM symbols) is copied as a cyclic prefix and inserted into the guard interval (GI) to form a block of $(N_f \times N_c + N_g)$ samples. This is illustrated in Fig. 2.

The orthogonal MC DS-CDMA block is transmitted over a frequency-selective fading channel and is received at a receiver. After the removal of GI, the received orthogonal MC DS-CDMA signal is decomposed by $N_f \times N_c$-point FFT into $N_f \times N_c$ frequency components. After performing FDE, $N_f \times N_c$-point IFFT is applied to obtain the time-domain MC DS-CDMA signal. This time-domain MC DS-CDMA signal is divided into a sequence of N_c-sample signal blocks. Then the orthogonal MC DS-CDMA demodulation is carried out as follows. The N_c subcarrier components of the OFDM signal are obtained by applying N_c-point FFT. Then, each subcarrier component is despread, followed by parallel/serial (P/S) conversion to obtain a sequence of decision variables for data demodulation.

Below, the transmission of one block is considered. Throughout the paper, sample-spaced discrete time signal representation is used.

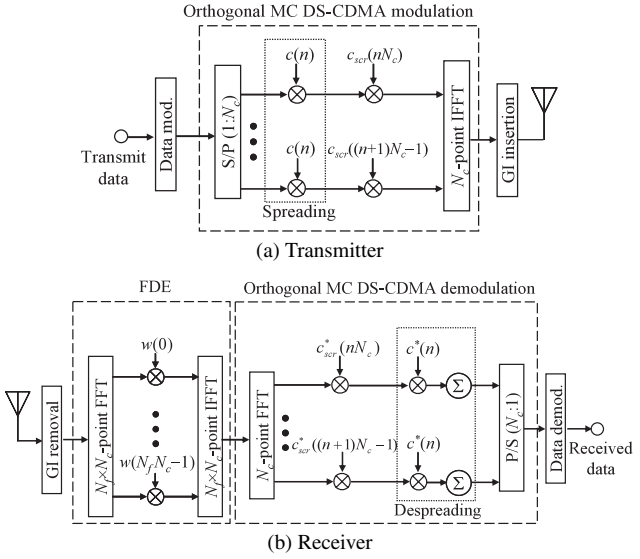

Fig. 1 Transmitter/receiver structure.

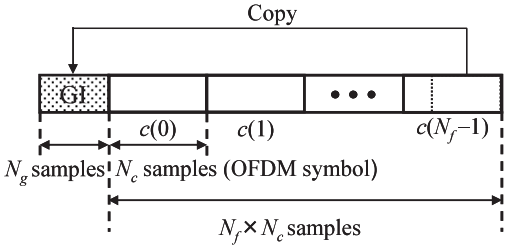

Fig. 2 Block structure.

2.2 Transmit Signal Representation

The orthogonal MC DS-CDMA signal $\{s(t);\ t = 0{\sim}\ N_f N_c - 1\}$ in one block interval can be expressed as

$$s(t) = \sqrt{\frac{2E_c}{T_c}}\, s\,(t \bmod N_c, \lfloor t/N_c \rfloor)\,, \tag{1}$$

where E_c and T_c denote the chip energy and chip period, respectively, and $\{s(t,\ n);\ t = 0\ {\sim}\ N_c{-}1\}$ is the orthogonal MC DS-CDMA signal in the nth chip interval, given as

$$s(t,n) = \sum_{i=0}^{N_c-1} S\,(n,i) \exp\left(j2\pi i \frac{t}{N_c}\right). \tag{2}$$

In Eq. (2), $S\,(n,i)$ is the ith subcarrier component and is given by

$$S\,(n,i) = d\,(\lfloor n/SF \rfloor\,, i)\, c(n \bmod SF) c_{scr}(i + nN_c), \tag{3}$$

where $\lfloor x \rfloor$ denotes the largest integer smaller than or equal to x, $d(m,i)$ is the mth symbol to be transmitted on the ith subcarrier, and $c_{scr}(i)$ is the scramble sequence (note that when $N_f < SF$, data symbol to be transmitted on each subcarrier is spread over more-than-one orthogonal MC DS-CDMA blocks). After the insertion of the GI, the orthogonal MC DS-CDMA signal is transmitted.

2.3 Received Signal Representation

The fading channel is assumed to have sample-spaced L discrete paths, each subjected to independent block fading. The assumption of block fading means that the path gains stay constant over at least one block duration. The impulse response $h(\tau)$ of multipath channel can be expressed as

$$h(\tau) = \sum_{l=0}^{L-1} h_l \delta(\tau - \tau_l), \tag{4}$$

where h_l and τ_l are the complex-valued path gain and time

delay of the lth path ($l = 0 \sim L-1$), respectively. In this paper, we assume exponential power delay profile with decay factor α as [2]

$$E[|h_l|^2] = \frac{1-\alpha^{-1}}{1-\alpha^{-L}}\alpha^{-l}. \tag{5}$$

The received MC DS-CDMA signal $\{r(t); t = 0 \sim N_f N_c - 1\}$ after removing the GI can be expressed as

$$r(t) = \sum_{l=0}^{L-1} h_l s((t-\tau_l) \bmod N_f N_c) + \eta(t), \tag{6}$$

where $\eta(t)$ is a zero-mean complex Gaussian process with variance $2N_0/T_c$ with N_0 being the single-sided power spectrum density of the additive white Gaussian noise (AWGN).

2.4 FDE

$N_f \times N_c$-point FFT is applied to decompose $\{r(t); t = 0 \sim N_f N_c - 1\}$ into $N_f \times N_c$ frequency components $\{R(k); k = 0 \sim N_f N_c - 1\}$. The kth frequency component $R(k)$ can be written as

$$\begin{aligned} R(k) &= \sum_{t=0}^{N_f N_c - 1} r(t) \exp\left(-j2\pi k \frac{t}{N_f N_c}\right), \\ &= H(k)S(k) + \Pi(k) \end{aligned} \tag{7}$$

where $S(k)$, $H(k)$ and $\Pi(k)$ are the kth frequency component of the transmitted MC DS-CDMA signal $\{s(t); t = 0 \sim N_f N_c - 1\}$, the channel gain, and the noise component due to the AWGN, respectively. They are given by

$$\begin{cases} S(k) = \displaystyle\sum_{t=0}^{N_f N_c - 1} s(t) \exp\left(-j2\pi k \frac{t}{N_f N_c}\right) \\ H(k) = \displaystyle\sum_{l=0}^{L-1} h_l \exp\left(-j2\pi k \frac{\tau_l}{N_f N_c}\right) \\ \Pi(k) = \displaystyle\sum_{t=0}^{N_f N_c - 1} \eta(t) \exp\left(-j2\pi k \frac{t}{N_f N_c}\right) \end{cases}. \tag{8}$$

FDE is carried out as

$$\hat{R}(k) = w(k)R(k) = \hat{H}(k)S(k) + \hat{\Pi}(k), \tag{9}$$

where $w(k)$ is the MMSE equalization weight, given by [8]

$$w(k) = \frac{H^*(k)}{|H(k)|^2 + (E_c/N_0)^{-1}}, \tag{10}$$

and

$$\begin{cases} \hat{H}(k) = w(k)H(k) \\ \hat{\Pi}(k) = w(k)\Pi(k) \end{cases}. \tag{11}$$

$N_f N_c$-point IFFT is applied to obtain the time-domain MC DS-CDMA signal $\{\hat{r}(t); t = 0 \sim N_f N_c - 1\}$ as

$$\hat{r}(t) = \frac{1}{N_f N_c} \sum_{k=0}^{N_f N_c - 1} \hat{R}(k) \exp\left(j2\pi k \frac{t}{N_f N_c}\right). \tag{12}$$

2.5 Despreading and Data Demodulation

The time-domain MC DS-CDMA signal $\{\hat{r}(t); t = 0 \sim N_f N_c - 1\}$ is divided into a sequence of N_c-sample signal blocks. N_c-point FFT is applied to decompose $\{\hat{r}(t); t = 0 \sim N_c - 1\}$ into N_c subcarrier components $\{\tilde{R}(n,i); i = 0 \sim N_c - 1\}$. The ith subcarrier component $\tilde{R}(n,i)$ can be written as

$$\begin{aligned} \tilde{R}(n,i) &= \frac{1}{N_c} \sum_{t=nN_c}^{(n+1)N_c - 1} \hat{r}(t) \exp\left(-j2\pi i \frac{t}{N_c}\right) \\ &= \sqrt{\frac{2E_c}{T_c}} \left(\frac{1}{N_f} \sum_{k=0}^{N_f N_c - 1} \hat{H}(k)\Phi^2(k,i) \right) S(n,i) \\ &\quad + \sqrt{\frac{2E_c}{T_c}} \Bigg(\frac{1}{N_f} \sum_{k=0}^{N_f N_c - 1} \hat{H}(k) \sum_{\substack{n'=0 \\ n' \neq n \text{ and } i' \neq i}}^{N_f - 1} \sum_{i'=0}^{N_c - 1} \\ &\qquad \exp\left(j\pi \left((N_c - 1)\frac{(i'-i)}{N_c} - 2k\frac{(n'-n)}{N_f} \right) \right) \\ &\qquad \times \Phi(k,i)\Phi(k,i')S(n',i') \Bigg) \\ &\quad + \frac{1}{N_f N_c} \sum_{k=0}^{N_f N_c - 1} \hat{\Pi}(k) \\ &\qquad \exp\left(j\pi \{(2n+1)N_c - 1\} \frac{k - N_f i}{N_f N_c} \right) \Phi(k,i), \end{aligned} \tag{13}$$

where the first term is the desired ith subcarrier component, the second is the inter-subcarrier interference (ISI), and the third is the noise. $\Phi(k,i)$ is defined as

$$\Phi(k,i) = \begin{cases} 1, & \text{if } k = N_f i \\ \dfrac{1}{N_c} \dfrac{\sin\left(\pi \frac{k - N_f i}{N_f}\right)}{\sin\left(\pi \frac{k - N_f i}{N_f N_c}\right)}, & \text{otherwise.} \end{cases} \tag{14}$$

As an example, $\Phi(k, i = 30)$ for $N_c = 64$, $N_f = 2$ and $i = 30$ is plotted in Fig. 3.

Despreading is carried out on $\tilde{R}(n,i)$, to obtain

$$\begin{aligned} \tilde{d}(m,i) &= \frac{1}{SF} \sum_{n=mSF}^{(m+1)SF - 1} \tilde{R}(n,i) \{c(n \bmod SF) c_{scr}(i + nN_c)\}^* \\ &= \sqrt{\frac{2E_c}{T_c}} \bar{H}(i) d(m,i) + \mu_{ISI}(m,i) + \mu_{noise}(m,i). \end{aligned} \tag{15}$$

Note that when $N_f < SF$, despreading is carried out over more-than-one orthogonal MC DS-CDMA blocks. $\tilde{d}(m,i)$ is the decision variable for data demodulation on $d(m,i)$, where

$$\bar{H}(i) = \frac{1}{N_f} \sum_{k=0}^{N_f N_c - 1} \hat{H}(k)\Phi^2(k,i). \tag{16}$$

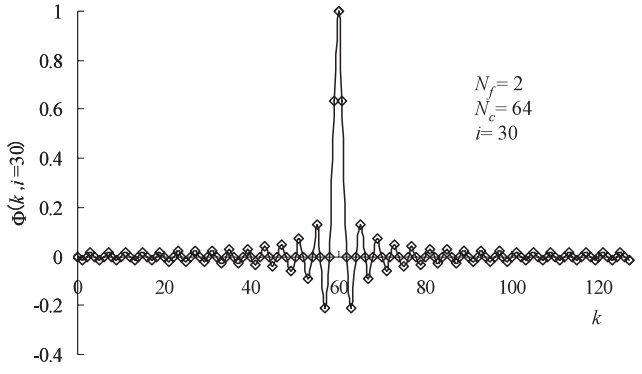

Fig. 3 $\Phi(k, i = 30)$ as a function of k.

$\bar{H}(i)$ is called the equivalent channel gain after FDE and despreading. The first term of Eq. (15) represents the data symbol, $\mu_{ISI}(m, i)$ is the ISI and $\mu_{noise}(m, i)$ is the noise. $\mu_{ISI}(m, i)$ and $\mu_{noise}(m, i)$ are given as

$$\mu_{ISI}(m,i) = \sqrt{\frac{2E_c}{T_c}}\frac{1}{N_f}\frac{1}{SF}\sum_{n=mSF}^{(m+1)SF-1}\sum_{k=0}^{N_fN_c-1}\hat{H}(k) \times \sum_{\substack{n'=0 \\ n'\neq n \text{ and } i'\neq i}}^{N_f-1}\sum_{i'=0}^{N_c-1}\left[\exp\left(j\pi\left((i'-i)\frac{(N_c-1)}{N_c}-2k\frac{(n'-n)}{N_f}\right)\right) \times \Phi(k,i)\Phi(k,i')S(n',i')\right] \times \{c(n \bmod SF)c_{scr}(i+nN_c)\}^*, \quad (17)$$

$$\mu_{noise}(m,i) = \frac{1}{N_fN_c}\frac{1}{SF}\sum_{n=mSF}^{(m+1)SF-1}\sum_{k=0}^{N_fN_c-1}\hat{\Pi}(k) \times \exp\left(j\pi\{(2n+1)N_c-1\}\frac{k-N_fi}{N_fN_c}\right)\Phi(k,i) \times \{c(n \bmod SF)c_{scr}(i+nN_c)\}^*. \quad (18)$$

In principle, the above described FDE process of DS-CDMA signal transmitted on a certain subcarrier is similar to the FDE process for single-carrier (SC) transmission [15] or single-carrier DS-CDMA [9]. However, it should be noted that since the received orthogonal MC DS-CDMA signal using N_c orthogonal subcarriers is decomposed by $N_f \times N_c$-point FFT into more-than-N_c frequency components, the inter-subcarrier interference is produced, thereby producing the ISI.

3. BER Analysis

Quateranary phase shift keying (QPSK) data modulation is assumed. The conditional BER is derived for the given $\{H(k);\ k = 0 \sim N_fN_c - 1\}$. Since $\mu_{ISI}(m, i)$ is the sum of many interference components, $\mu_{ISI}(m, i)$ can be approximated, according to the central limit theorem [16], as a zero-mean complex Gaussian variable. Therefore, the sum of $\mu_{ISI}(m, i)$ and $\mu_{noise}(m, i)$ can be treated as a zero-mean complex Gaussian variable $\mu(m, i)$. As a consequence, $\tilde{d}(m, i)$ of Eq. (15) becomes a complex Gaussian variable with mean $\sqrt{\frac{2E_c}{T_c}}\left(\frac{1}{N_f}\sum_{k=0}^{N_fN_c-1}\hat{H}(k)\Phi^2(k,i)\right)d(m,i)$ and variance $2\sigma_\mu^2(i)$. $2\sigma_\mu^2(i)$ is given as

$$2\sigma_\mu^2(i) = \frac{1}{SF}\frac{2E_c}{T_c}\left[\frac{1}{N_f}\left(\sum_{k=0}^{N_fN_c-1}\left|\hat{H}(k)\right|^2\Phi^2(k,i)\left(\sum_{i'=0}^{N_c-1}\Phi^2(k,i')\right)\right) - \left|\frac{1}{N_f}\sum_{k=0}^{N_fN_c-1}\hat{H}(k)\Phi^2(k,i)\right|^2\right] + \frac{1}{SF}\frac{2N_0}{T_c}\frac{1}{N_fN_c}\left(\sum_{k=0}^{N_fN_c-1}|w(k)|^2\Phi^2(k,i)\right), \quad (19)$$

The conditional signal-to-interference plus noise power ratio (SINR) $\gamma(E_s/N_0, \{H(k)\})$ is given by

$$\gamma\left(\frac{E_s}{N_0},\{H(k)\}\right) = \frac{\frac{2E_c}{T_c}\left|\frac{1}{N_f}\sum_{k=0}^{N_fN_c-1}\hat{H}(k)\Phi^2(k,i)\right|^2}{\sigma_\mu^2(i)} = \frac{\frac{2E_s}{N_0}\left|\frac{1}{N_f}\sum_{k=0}^{N_fN_c-1}\hat{H}(k)\Phi^2(k,i)\right|^2}{\frac{1}{SF}\cdot\frac{E_s}{N_0}\left[\frac{1}{N_f}\left(\sum_{k=0}^{N_fN_c-1}\left|\hat{H}(k)\right|^2\Phi^2(k,i)\left(\sum_{i'=0}^{N_c-1}\Phi^2(k,i')\right)\right) - \left|\frac{1}{N_f}\sum_{k=0}^{N_fN_c-1}\hat{H}(k)\Phi^2(k,i)\right|^2\right] + \frac{1}{N_fN_c}\left(\sum_{k=0}^{N_fN_c-1}|w(k)|^2\Phi^2(k,i)\right)}, \quad (20)$$

where E_s $(=E_c \cdot SF)$ is the data symbol energy. The conditional BER for QPSK modulation is given by [2]

$$p_b\left(\frac{E_s}{N_0},\{H(k)\}\right) = \frac{1}{2}\mathrm{erfc}\left[\sqrt{\frac{1}{4}\gamma\left(\frac{E_s}{N_0},\{H(k)\}\right)}\right], \quad (21)$$

where $\mathrm{erfc}[x] = \left(2/\sqrt{\pi}\right)\int_x^\infty \exp(-t^2)dt$ is the complementary error function. The theoretical average BER $P_b(E_s/N_0)$ can be numerically evaluated by averaging Eq. (21) over all realizations of $\{H(k); k = 0 \sim N_fN_c - 1\}$.

4. Numerical Computation and Computer Simulation

4.1 Numerical and Simulation Conditions

Table 1 summarizes the numerical and simulation conditions. The fading channel is assumed to be a frequency-selective block Rayleigh fading channel having a sample-spaced $L = 16$-path exponential power delay profile with decay factor α. Ideal channel estimation is assumed. If a

Table 1 Numerical and simulation conditions.

Data modulation		QPSK
MC DS-CDMA	No. of subcarriers	N_c=64
	Spreading factor	SF=1~64
	Spreading sequence	Walsh-Hadamard
	Code multiplexing order	C=1~64
	Block size	N_f=1~8
	No. of GI length	N_g=16
Channel model	Fading	Frequency-selective Block Rayleigh fading
	No. of paths	L=16
	Power delay profile	Exponential power delay profile
	Decay factor	α=0, 2, 4, 6, ∞dB
FDE	Channel estimation	Ideal
	weight	MMSE
	FFT/IFFT size	N_fN_c=64~512

100 MHz bandwidth (i.e., a chip rate of 1.56 Mcps for each subcarrier) in the 5 GHz band is assumed as in [17], the GI length and the root-mean-square (RMS) delay spread τ_{rms} are respectively given by 0.16 μs and $\tau_{rms} \approx 0.046\,\mu$s when $\alpha = 0$ dB.

4.2 Single-Code Case ($C = 1$)

Figure 4 plots the BER performance of orthogonal MC DS-CDMA using FDE with the block size N_f as a parameter. A fairly good agreement between the theoretical and simulated results is seen. The BER performance is improved by increasing N_f because the frequency diversity gain increases. However, additional performance improvement cannot be seen when $N_f \geq 4$. The reason for this is discussed below.

The equivalent channel gain $\bar{H}(i)$ after FDE and despreading, given by Eq. (16), is a weighted sum of $\hat{H}(k)'s$. Figure 5 plots one shot example of $\hat{H}(k)$ and $\Phi^2(k, i = 30)$ with $N_f = 2$ and 4 for the case of $N_c = 64$ and $\alpha = 0$ dB. $\Phi^2(k, i = 30)$ has its peak of 1 at $k = i \times N_f$ and decays rapidly when $k \neq i \times N_f$ (when $N_f = 2$, the subcarrier $i = 30$ corresponds to the frequency $k = 60$ for FDE). Figure 5 suggests that when $N_f = 2$ (4), the 3rd (7th)-order frequency diversity is achieved. But, the diversity gain depends on the fading correlation ρ between the adjacent frequencies k and $k + 1$. ρ is given, from Eq. (5) as [2]

$$\rho = \frac{(1/2)E[H^*(k)H(k+1)]}{\sqrt{(1/2)E[|H(k)|^2]}\sqrt{(1/2)E[|H(k+1)|^2]}} = \frac{1-\alpha^{-1}}{1-\alpha^{-L}}\sum_{l}^{L-1}\alpha^{-l}\exp\left(-j2\pi\frac{\tau_l}{N_fN_c}\right). \quad (22)$$

As N_f increases, ρ increases for the given values of N_c and α. This offsets the diversity gain increase obtainable by the increase of the diversity order.

Figure 6 plots the BER performance with the decay factor α as a parameter. A fairly good agreement between the theoretical and simulated results is seen. The BER performance degrades as α increases. This performance degradation is due to the increase of ρ as α increases as shown in

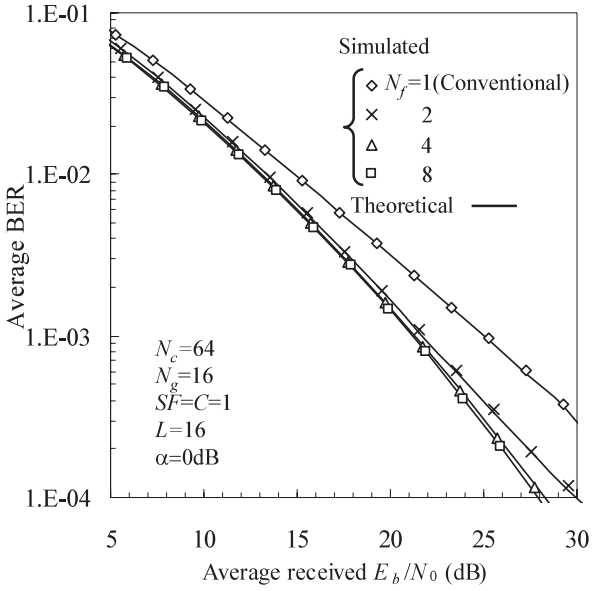

Fig. 4 Impact of block size N_f.

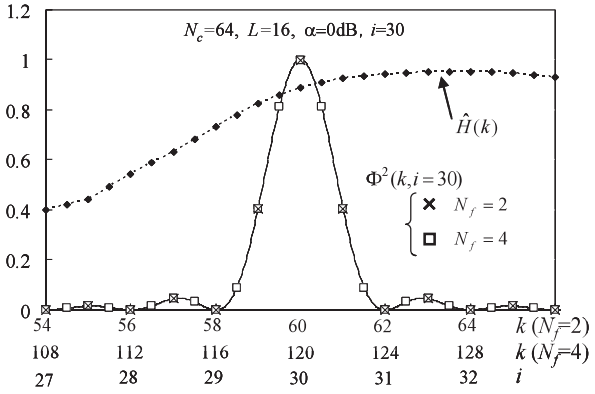

Fig. 5 $\hat{H}(k)$ and $\Phi^2(k, i = 30)$.

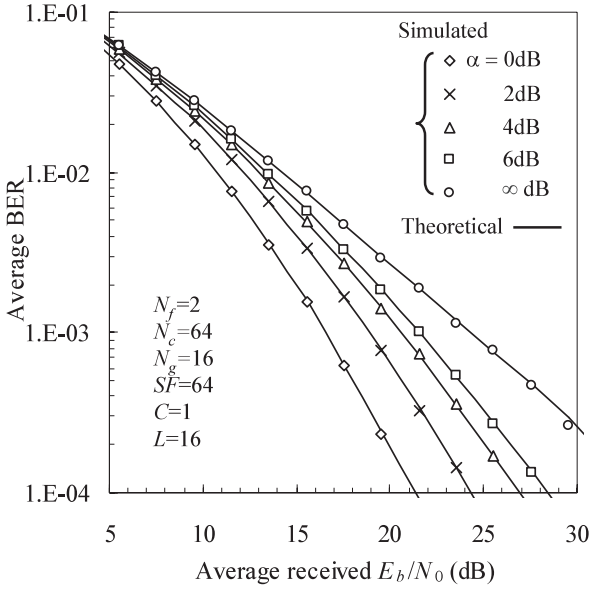

Fig. 6 Impact of decay factor α.

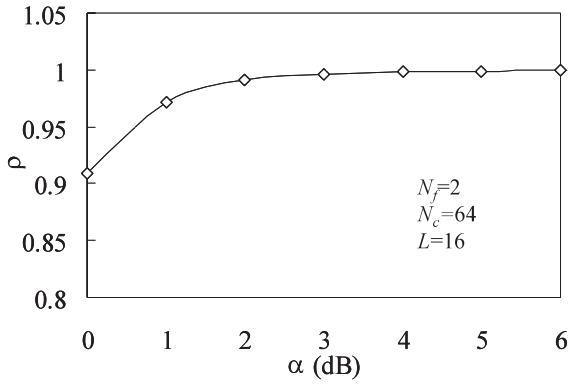

Fig. 7 Impact of α on ρ.

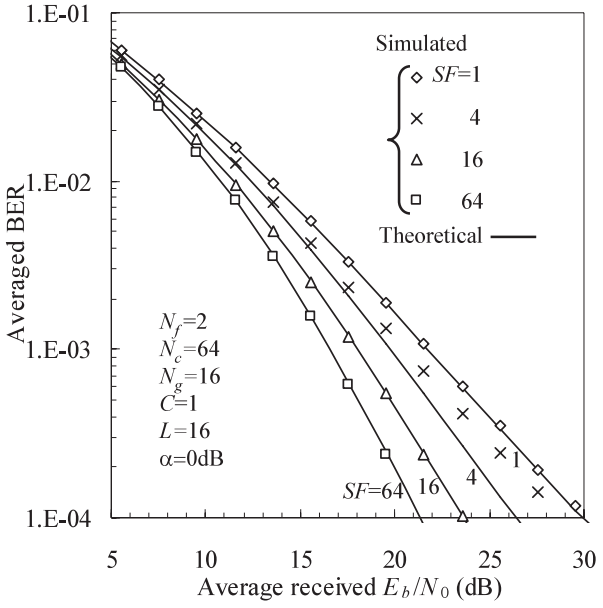

Fig. 8 Impact of SF.

Fig. 7.

Figure 8 shows the BER performance with SF as a parameter. The BER performance improves by increasing SF, since the residual ISI can be sufficiently suppressed. Our theoretical analysis is based on the Gaussian approximation of the ISI (see Sect. 3). The deviation of the theoretical performance from the simulation result is due to the fact that the ISI cannot be well approximated by the Gaussian distribution when $SF = 4$.

4.3 Multi-Code Case

So far we have considered the single-code orthogonal MC DS-CDMA. Orthogonal code multiplexing can be used to increase the transmission data rate. Figure 9 plots the BER performance with the code-multiplexing order C as a parameter when $SF = 64$. Similar to Sect. 3, we have derived the received SINR expression for the multi-code case. The SINR is given by (its derivation is omitted for the sake of brevity)

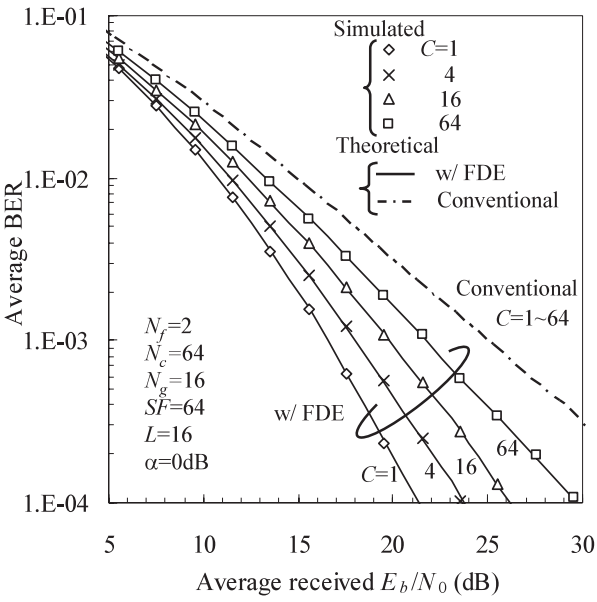

Fig. 9 Impact of code-multiplexing order C.

$$
\begin{aligned}
&\gamma\left(\frac{E_s}{N_0},\{H(k)\}\right)\\
&=\frac{\dfrac{2E_s}{N_0}\left|\dfrac{1}{N_f}\displaystyle\sum_{k=0}^{N_fN_c-1}\hat{H}(k)\Phi^2(k,i)\right|^2}{\dfrac{C}{SF}\cdot\dfrac{E_s}{N_0}\left[\dfrac{1}{N_f}\left(\displaystyle\sum_{k=0}^{N_fN_c-1}\left|\hat{H}(k)\right|^2\Phi^2(k,i)\left(\sum_{i'=0}^{N_c-1}\Phi^2(k,i')\right)\right)-\left|\dfrac{1}{N_f}\displaystyle\sum_{k=0}^{N_fN_c-1}\hat{H}(k)\Phi^2(k,i)\right|^2\right]+\dfrac{1}{N_fN_c}\left(\displaystyle\sum_{k=0}^{N_fN_c-1}|w(k)|^2\Phi^2(k,i)\right)},
\end{aligned}
\tag{23}
$$

from which the theoretical BER performance was evaluated. A fairly good agreement between the theoretical and simulated results is seen. As C increases, the BER performance degrades and approaches that of the conventional orthogonal MC DS-CDMA ($N_f = 1$). In our orthogonal MC DS-CDMA, the frequency-nonselective channel cannot be perfectly restored by using MMSE-FDE and therefore, the ISI is produced as shown in Eq. (15). As a consequence, as C increases, the BER performance degrades. However, even for $C = 64$ (full code-multiplexing), the BER performance is still better than the conventional orthogonal MC DS-CDMA as seen from Fig. 9 (note that the BER performance of the conventional orthogonal MC DS-CDMA is the same for all C).

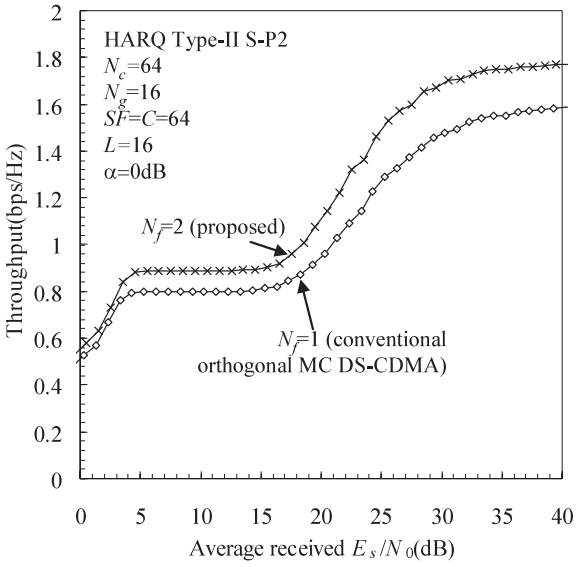

Fig. 10 Throughput performance.

4.4 Throughput Performance of HARQ Using IR Strategy

So far, we have assumed the uncoded case and evaluated the BER performance of orthogonal MC DS-CDMA with FDE. However, in practical systems, some form of error control technique is indispensable. Here, we consider HARQ using IR strategy, which transmits uncoded packet at initial transmission and then, parity check packet is transmitted if retransmission is requested. As the number of retransmissions increase, the error correction capability gets stronger. Since the initial packet transmission is uncoded, no coding gain can be expected. Orthogonal MC DS-CDMA using FDE can achieve the frequency diversity gain even without channel coding and can improve the throughput performance of HARQ using IR strategy. We consider the turbo-coded HARQ type-II with S-P2 [14] as an example of HARQ using IR strategy. When 100 MHz bandwidth (i.e., a chip rate of 1.56 Mcps and $N_c = 64$ subcarriers), the maximum throughput reaches about 177 Mbps (1.77 bps/Hz) with $N_f = 2$ for the full code-multiplexing ($SF = C$). Figure 10 plots the throughput performance for the full code-multiplexing case ($SF = C = 64$). It is seen from Fig. 10 that the orthogonal MC DS-CDMA with FDE can achieve a better throughput performance than the conventional orthogonal MC DS-CDMA. The throughput improvement is due to the frequency-diversity gain and the reduction of GI insertion rate (the GI insertion rate is halved for $N_f = 2$).

5. Conclusion

In this paper, we proposed the technique of orthogonal MC DS-CDMA with FDE, which can obtain the frequency diversity gain and hence can improve the BER performance. The average BER analysis of the proposed orthogonal MC DS-CDMA in a frequency-selective Rayleigh fading channel was presented and was confirmed by computer simulation. It was shown that the proposed orthogonal MC DS-CDMA provides better BER performance than the conventional orthogonal MC DS-CDMA even for the full code-multiplexing case.

In this paper, we proposed orthogonal MC DS-CDMA using FDE to get the frequency diversity gain. Another way to get the frequency diversity (or the path diversity) gain is to apply the well-known rake combining on each subcarrier [18]. The achievable transmission performance depends on the modulation bandwidth of each subcarrier. The performance comparison between using FDE and rake combining is lest as an interesting future study.

References

[1] W.C. Jakes, Jr., ed, Microwave mobile communications, Wiley, New York, 1974.
[2] J.G. Proakis, Digital communications, 2nd ed., McGraw-Hill, 1995.
[3] Y. Akaiwa, Introduction to digital mobile communication, Wiley-Interscience, 1997.
[4] H. Meyr, M. Moeneclaey, and S.A. Fechtel, Digital communication receivers, Wiley-Interscience, 1998.
[5] L. Hanzo, W. Webb, and T. Keller, Single- and Multi-carrier Quadrature Amplitude Modulation, Wiley, 2000.
[6] S. Hara and R. Prasad, "Overview of multicarrier CDM," IEEE Commun. Mag., vol.35, no.12, pp.126–133, Dec. 1997.
[7] S. Hara and R. Prasad, "Design and performance of multicarrier CDMA system in frequency-selective Rayleigh fading channels," IEEE Trans. Veh. Technol., vol.48, no.5, pp.1584–1595, Sept. 1999.
[8] T. Sao and F. Adachi, "Comparative study of various frequency equalization techniques for downlink of a wireless OFDM-CDMA system," IEICE Trans. Commun., vol.E86-B, no.1, pp.352–364, Jan. 2003.
[9] F. Adachi, D. Garg, S. Takaoka, and K. Takeda, "Broadband CDMA techniques," IEEE Wireless Commun. Mag., vol.12, no.2, pp.8–18, April 2005.
[10] S. Tomasin and N. Benvenuto, "Frequency-domain interference cancellation and nonlinear equalization for CDMA systems," IEEE Trans. Commun., vol.4, no.5, pp.2329–2339, Sept. 2005.
[11] H. Atarashi, A. Abeta, and M. Sawahashi, "Variable spreading factor-orthogonal frequency and code division multiplexing (VSF-OFCDM) for broadband packet wireless access," IEICE Trans. Commun., vol.E86-B, no.1, pp.291–299, Jan. 2003.
[12] N. Maeda, Y. Kishihara, H. Atarashi, and M. Sawahashi, "Variable spreading factor-OFCDM with two dimensional spreading that prioritizes time domain spreading for forward link broadband wireless access," IEICE Trans. Commun., vol.E88-B, no.2, pp.487–498, Feb. 2005.
[13] D.N. Rowitch and L.B. Milstein, "Rate compatible punctured turbo (RCPT) codes in hybrid FEC/ARQ system," Proc. Comm. Theory Mini-conference of GLOVECOM'97, pp.55–59, Nov. 1997.
[14] D. Garg and F. Adachi, "Throughput comparison of turbo-coded HARQ in OFDM, MC-CDMA and DS-CDMA with frequency-domain equalization," IEICE Trans. Commun., vol.E88-B, no.2, pp.664–677, Feb. 2005.
[15] D. Falconer, S.L. Ariyavisitakul, A. Benyamin-Seeyar, and B. Eidson, "Frequency domain equalization for single-carrier broadband wireless systems," IEEE Commun. Mag., vol.40, no.4, pp.58–66, April 2002.
[16] A. Papoulis and S.U. Pillai, Probability, Random Variable and Stochastic Processes, McGraw-Hill Higher Education, 2002.
[17] H. Taoka, K. Higuchi, and M. Sawahashi, "Field experiments on 2.5-Gbps packet transmission using MLD-based signal detection in

MIMO-OFDM broadband packet radio Aaccess," Proc. 9th WPMC, pp.234–239, San Diego, USA, Sept. 2006.

[18] L.-L. Yang and L. Hanzo, "Performance of generalized multicarrier DS-CDMA over Nakagami-m fading channels," IEEE Trans. Commun., vol.50, no.6, pp.956–966, June 2002.

Ken Tanaka received his B.S. and M.S. degrees in communications engineering from Tohoku University, Sendai, Japan, in 2005 and 2007, respectively. Since April 2007, he has been with Denso Corporation. His research interests include multi-carrier direct sequence code division multiple access technique and frequency-domain equalization for mobile communication systems.

Hiromichi Tomeba received his B.S. and M.S. degrees in communications engineering from Tohoku University, Sendai, Japan, in 2004 and 2006. Currently he is a Japan Society for the Promotion of Science (JSPS) research fellow, studying toward his PhD degree at the Department of Electrical and Communications Engineering, Graduate School of Engineering, Tohoku University. His research interests include frequency-domain equalization and antenna diversity techniques for mobile communication systems. He was a recipient of the 2004 and 2005 IEICE RCS (Radio Communication Systems) Active Research Award.

Fumiyuki Adachi received the B.S. and Dr. Eng. degrees in electrical engineering from Tohoku University, Sendai, Japan, in 1973 and 1984, respectively. In April 1973, he joined the Electrical Communications Laboratories of Nippon Telegraph & Telephone Corporation (now NTT) and conducted various types of research related to digital cellular mobile communications. From July 1992 to December 1999, he was with NTT Mobile Communications Network, Inc. (now NTT DoCoMo, Inc.), where he led a research group on wideband/broadband CDMA wireless access for IMT-2000 and beyond. Since January 2000, he has been with Tohoku University, Sendai, Japan, where he is a Professor of Electrical and Communication Engineering at the Graduate School of Engineering. His research interests are in CDMA wireless access techniques, equalization, transmit/receive antenna diversity, MIMO, adaptive transmission, and channel coding, with particular application to broadband wireless communications systems. From October 1984 to September 1985, he was a United Kingdom SERC Visiting Research Fellow in the Department of Electrical Engineering and Electronics at Liverpool University. He was a co-recipient of the IEICE Transactions best paper of the year award 1996 and again 1998 and also a recipient of Achievement award 2003. He is an IEEE Fellow and was a co-recipient of the IEEE Vehicular Technology Transactions best paper of the year award 1980 and again 1990 and also a recipient of Avant Garde award 2000. He was a recipient of Thomson Scientific Research Front Award 2004.